Development of an Extremely Lightweight, High-Altitude Decelerator

PETER G. NIEDERER*
Astro Research Corporation, Santa Barbara, Calif.

This paper describes work aimed at developing a parachute that will allow meteorological probes to descend from very high altitudes at subsonic velocities. By making a parachute fabric of thin tapes which are widely spaced, over-all drag coefficients up to unity based on canopy projected area are achieved with a mesh solidity of 0.2. Such designs take advantage of the high drag coefficients obtained in very low Reynolds number flow, the so-called Stokes-flow regime. The results of subscale drop tests through vacuum chambers are in reasonable agreement with theory. Configurations using this principle are described. The problem of supplying the necessary external bracing by means of inflatable tubes is discussed, and weight and performance studies are outlined. The studies suggest, for example, that a parachute of 49-m^2 projected canopy area would have a mass of 0.5 kg and would provide a drag coefficient of 0.7, a ballistic coefficient (with 2.0-kg payload) of 0.074 kg/m^2, and the ability for subsonic descent from ~80-km altitude.

Nomenclature

A = projected area of parachute
A' = surface area of canopy
C_D = drag coefficient of parachute, D/q_0A
C_{D_1} = drag coefficient of flat tape, D_1/q_1d; C_{D_1c} is corrected to include rarefied gas effects
C_{D_f} = drag coefficient of flat tape in free molecular flow
D = drag force of parachute
D_1 = drag force per unit length of flat tape
d = width of tape
E = modulus of elasticity
h = centerline-to-centerline spacing of tapes
J = moment of inertia
Kn_d = λ/d = Knudsen number
l = length of brace, center to tip
M_1 = Mach number of flow through canopy
M_w = critical bending moment for wrinkling of inflated tube
m = total system mass
m_c,m_p = parachute and payload masses, respectively
b = m/AC_D = ballistic coefficient
p = internal pressure in brace
q = dynamic pressure, $\rho v^2/2$
Re_d = Reynolds number based on tape width, $dv\rho/\mu$
r = radius of brace tube
t = tube wall thickness for brace
v = velocity
W = total system weight, g
α = canopy rise angle
ϵ = solidity of mesh, $2d/h$ if $h \gg d$
ρ = air density
σ = hoop stress

Subscripts

0 = freestream conditions
1 = local flow conditions through canopy

Introduction

METEOROLOGICAL research of the altitudes between 50 and 100 km above the earth's surface depends to a large extent on comparatively small sounding rockets, such as the Loki-Dart and Arcas systems, with payloads of 0.5 to 7 kg. Near the rocket's apogee, the instrument package is released and then decelerated by a parachute which descends slowly through the operating environment. Ideally, the parachute should have the following characteristics: 1) the ability to operate at subsonic descent speeds at high altitudes (e.g., up to 100 km); 2) rapid and reliable deployment, using a deployment aid if necessary; 3) aerodynamic stability; 4) radar reflectivity for ground-tracking purposes; 5) low production cost; and 6) ease of handling.

Advances in the state-of-the-art of high-altitude decelerators are generally recent. The earlier silk or nylon parachutes of circular or elliptic shape operated with a mesh porosity low enough and at dynamic pressures high enough that they could be deployed and supported by the internal pressure in the canopy.[1] The introduction of very thin polyester-type films opened new possibilities for improving the performance of high-altitude parachutes, and the following types show marked improvements in aerodynamic stability and permit subsonic descent from altitudes of 50 to 60 km.

1) The "disk-gap-band" (DGB) parachute[2] uses a flat, circular disk of scrim-reinforced Mylar foil, with no porosity, to generate a high drag coefficient with a minimum of material. Aerodynamic stability of the canopy is achieved by use of geometric porosity provided by a circular gap around the disk.

2) The "Ballute,"† as developed for the Loki-Dart system,[3] consists of a square-shaped truncated cone of quarter-mil Mylar and is inflated by ram-air. The payload is swivel-suspended immediately below the air inlet.

This paper describes an extremely lightweight decelerator, the Stokes-flow parachute,[4,5] which utilizes the well-known fact that a very thin filament experiences a high viscous drag force at small Reynolds numbers based on its width, e.g., $Re_{d1} < 1$. An aerodynamic theory has been developed which indicates that even a very tenuous mesh of widely spaced filaments produces over-all drag coefficients up to unity at an extremely low weight per unit area. Figure 1 shows two typical Stokes-flow parachute concepts. In each case the canopy shape approximates a flat plate or disk, but some billowing must be allowed to avoid excessive stresses and compressive forces in the disk. The canopy consists of an open mesh of thin Mylar tapes; its solidity is typically from 10 to 30%.

Presented as Paper 68-949 at the AIAA 2nd Aerodynamic Deceleration Systems Conference, El Centro, Calif., September 23–25, 1968; submitted November 4, 1968; revision received August 21, 1969. This research was supported during 1966 by the NASA Goddard Space Flight Center (Contract NAS5-10168), and during 1968 by NASA Langley Research Center (Contract NAS1-7770).

* Aerodynamics Engineer.

† Trademark of Goodyear Aerospace Corp.

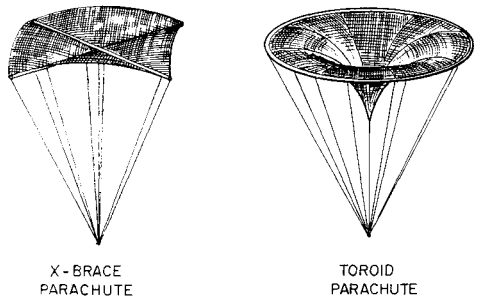

Fig. 1 Stokes-flow parachute concepts.

Since the airflow through this porous mesh does not develop enough internal pressure to deploy the parachute and to keep it erect, a compression-resistant structure is required for these functions. The X-brace and the toroidal brace of the parachutes shown in Fig. 1 preferably consist of thin-walled tubes that are inflated by a suitable pressurizing substance, e.g., water, methanol, Freon 11, or isopentane, packaged as a liquid that vaporizes at altitude. During descent of the deployed parachute, the overpressure in the brace tubes gradually decreases until the braces start to collapse. The payload is suspended below the canopy by a number of suspension lines distributed along the braces.

Figure 2 compares curves of b vs payload for various parachutes. The b for a hand-packaged Stokes-flow parachute is $\sim\frac{1}{3}$ that of a conventional system. Further improvement is indicated if pressure procedures are developed for packaging the canopies. Table 1 gives some approximate data for typical Stokes-flow parachutes as compared to currently operational parachutes.

Aerodynamic Theory and Initial Experiments

The theoretical approach taken in determining the drag coefficient of an open-mesh parachute is a modification of propeller theory, known as actuator disk theory,[6] which describes the increase of momentum of the airflow through the thrust-producing disk of a propeller. In the application of this theory to the Stokes-flow parachute, its canopy is represented by a drag-producing disk that causes a loss of momentum of the air flow passing through its area.

Similar to the Stokes-flow sphere, a thin filament produces arbitrarily high drag coefficients inversely proportional to Reynolds number. We combine this high viscous drag phenomenon, applied locally, with momentum flow through the entire drag-producing area A consisting of an array of many slender, widely spaced filaments. The local effective velocity v_1 in which the single filaments are immersed, is smaller than the freestream velocity v_0 due to a blocking effect of the fibers present;

$$v_1/v_0 = [1 + (1 - C_D)^{1/2}]/2 \qquad (1)$$

where $C_D = 2D/\rho v_0^2 A$. The fluid is assumed to be incompressible, and identical flow conditions are assumed throughout the area A. If the formula for the drag force developed by the entire disk A is equated to the formula of the sum of all local drag forces of the mesh elements, the expression

$$C_D = C_{D_1}(v_1/v_0)^2\epsilon \qquad (2)$$

is obtained. The variation of $C_{D_1}(= 2D_1/\rho v_1^2 d)$ with the local Reynolds number Re_{d_1} for various local Mach numbers M_1 is shown in Fig. 3. The curve for continuous flow at $Re_{d_1} < 0.3$ is described by the well-known Oseen formula,[7] which merges gradually into an experimentally determined value of 1.98 for high Re_{d_1}. Figure 4 shows C_D vs Re_{d_0} for various ϵ's. These curves, obtained with Eqs. (1) and (2) and Fig. 3, are for purely continuous flow conditions. The striking feature is that $C_D \simeq 1$ can be obtained for any low mesh solidity if Re_{d_0} is small enough. This C_D compares with an experimental value of 1.17 for a solid flat plate.

The initial experimental tests of the foregoing theory were done with small mesh models. Extremely thin fibers were required to simulate sufficiently low Reynolds numbers. The drag forces to be measured were so low (typically 0.5 to 5×10^{-4} N) that recording them with a balance in a wind-tunnel setup would have been difficult. Therefore, the models were dropped through a vacuum chamber, and their falls were recorded photographically using multiple exposures obtained by stroboscopic illumination. The drag coefficients were deduced from the descent rates and chamber pressures. The drop-test chamber was a tube 0.5 m in diameter and 1.8 m high which can be evacuated to pressures ranging from 0.5 to 760 torr. The models, with canopy diameters up to 7 cm, were either released from zero velocity or expelled by a pneumatically driven air gun placed axially above the chamber. Initial velocities up to 15 m/sec have been achieved. In the testing, a little ball of plasteline placed in the center of the mesh was required to balance the model and to improve the visibility of the photographs.

Figure 5 is a summary of drop test results with an electroformed nickel mesh having $\epsilon = 0.068$ and a single-fiber width of $d = 0.044$ mm. The total mass was 49.8 mg. The test

Table 1 Comparison of payload delivery systems for Arcas and Dart sounding rockets

Parameter	Arcas		Dart	
	C^a	S^a	C	S
Total system mass m, kg	5.6	4.2	0.50	0.42
Parachute mass m_c, kg	2.0	0.6	0.14	0.06
Payload mass m_p, kg	3.6	3.6	0.36	0.36
Projected canopy area A, m^2	11.0	50.0	3.5	10.0
Drag coefficient C_D	0.9	0.7	0.9	0.7
Ballistic coefficient b, kg/m^2	0.5	0.12	0.16	0.06

[a] C = currently operational parachute; S = Stokes-flow parachute.

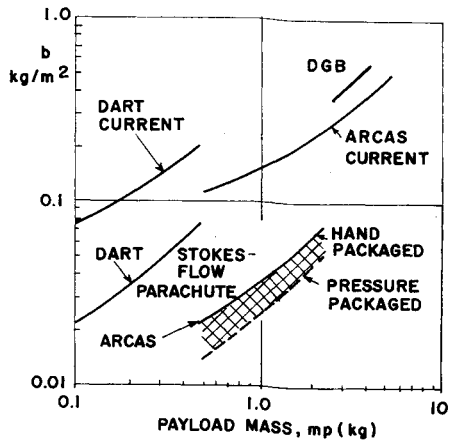

Fig. 2 Ballistic coefficient b for Arcas and Dart payload delivery systems.

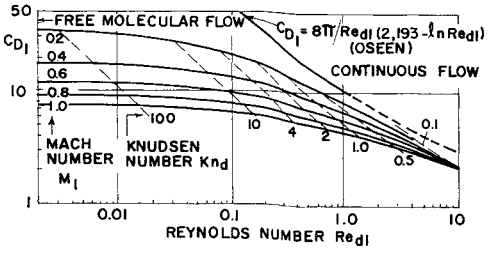

Fig. 3 Flat-tape drag coefficient C_{D1} in normal flow.

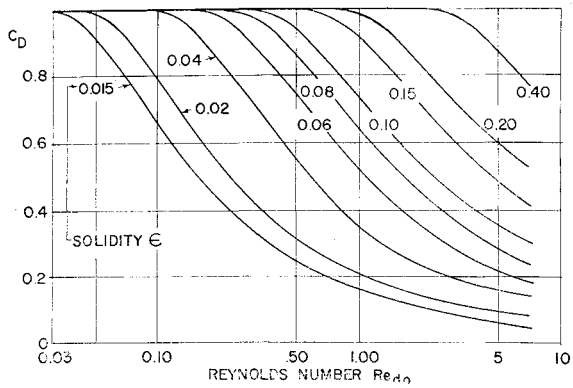

Fig. 4 Theoretical canopy drag coefficient curves for various solidities.

points indicate a qualitative confirmation of the features predicted by theory. (The scatter limits indicated were derived from an error analysis.) However, the test points generally lie above the theoretical curve. They seem to indicate that theory should be corrected for over-all Reynolds number effects for the small models tested, since C_D of a solid disk increases at the low end of the Reynolds number scale to values substantially larger than unity.[8]

In high-altitude operation, the mean free path of air is no longer negligible when compared with the width d of the tapes. It is, however, assumed small when compared to the size of the whole decelerator; thus, actuator disk theory is still applicable. The correction to account for rarefied gas effects is then applied to the local C_{D_1} of a single tape. The correction is included in Fig. 3 with the Mach number chosen as suitable parameter, described by Kn and Re[9];

$$M_1 = 0.67\ Kn_d Re_{d_1} \tag{3}$$

To the left of Fig. 3, free molecular flow conditions[9,10] (diffuse reflection) prevail. The drag coefficients for the slip flow regime are estimated by applying a matched correction to the drag coefficient in continuum flow,

$$C_{D_{1C}} = C_{D_1}/(1 + C_{D_f}^{-1}) \tag{4}$$

where C_{D_f} is a function of M_1 in free molecular flow conditions.[9]

The solid curves in Fig. 6 represent actuator disk theory including rarefied gas effects. Figure 6 shows C_D vs d for various ϵ's at $M_0 = 1$ at 80 km. The dotted line for $\epsilon = 0.1$ represents actuator disk theory without correction (Fig. 4); thus, the rarefied gas correction for $\epsilon = 0.1$ is represented by the shaded area.

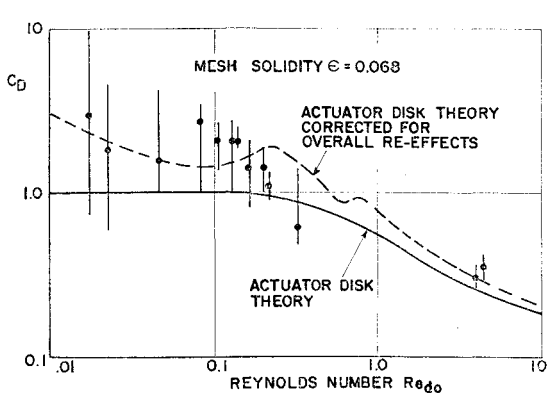

Fig. 5 Experimental results from drop tests with small mesh models.

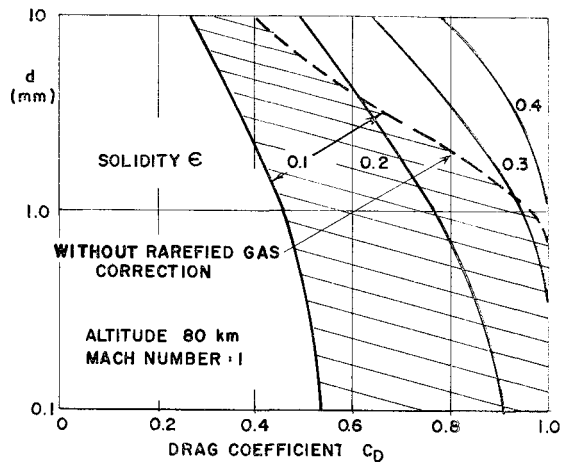

Fig. 6 Theoretical canopy drag coefficients including rarefied gas corrections.

Parachute Structural Design

The X-brace parachute (see Fig. 1) consists of a square canopy deployed and rigidized by two thin-walled inflated tubes, fixed diagonally to the square network. Its four sails between adjacent brace legs bulge out at an angle α between the midline of the sail and its projection in the plane of the braces (see Fig. 7). The payload is suspended from a number of suspension lines originating along the brace tubes. The aerodynamic loading of the canopy is approximated by the following assumptions: 1) the canopy consists of four sets of single parallel tapes running between adjacent brace legs, 2) the drag force produced per unit area is constant over the entire canopy, and 3) all the drag forces are parallel to the freestream direction. Because of these assumptions, each brace leg is loaded in bending and in compression by linearly distributed continuous force distribution as illustrated in Fig. 7. The transverse loads on one brace leg add up to a quarter of the total system weight W. The total compressive force is described by

$$P = [(2)^{1/2}/16]W/\tan\alpha \tag{5}$$

For all practical purposes, the compressive loading due to the angularity of the suspension lines can be neglected if their length is at least $3l$, or 1.5 times the length of the diagonal of the canopy.

If the brace is supported by a large number of suspension lines, the bending moments due to transverse loading become insignificant, and the only loading is in compression according to Eq. (5). The lowest buckling mode of each brace is then in-plane and each brace leg assumes a bowed shape. A limited number of suspension lines is, however, desirable to minimize tangling during deployment. The bending moments due to transverse loading are then dominant for moderate canopy rise angles.

The detailed load analysis[4] shows that at least three suspension lines are required for each brace leg. Their positions are in the center of the canopy, at the ends of the braces, and

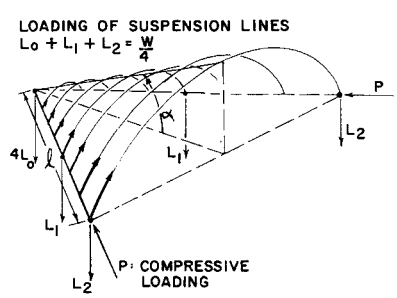

Fig. 7 X-brace loading conditions for structural estimates.

Table 2 Design parameters for X-brace parachutes of Fig. 8

Parameter	Arcas	Dart
Total system mass m, kg	2.5	0.49
Design altitude H, km	80	
Ballistic coefficient b, kg/m²	0.074	
Aluminized Mylar canopy thickness, mil	0.25	
Width of tapes d, mm	2	
Number of suspension lines	9	
Canopy rise angle α, deg	25	
Mylar brace tube wall thickness t, mil	0.5	0.333
Tube hoop stress σ, 10^7 N/m²	1.75	1.75

two-thirds of the distance toward the ends. The payload is then carried by a total number of nine lines. In this configuration, maximum bending moment occurring is

$$M_{max} < Wl \cdot 10^{-3}[6.78 + 0.00102Wl^2/(JE \tan\alpha)] \quad (6)$$

The brace is designed to carry a maximum moment without wrinkling

$$M_w = (\pi/2)pr^3 \quad (7)$$

The wall thickness t required in terms of tube radius and hoop stress σ is then

$$10^3 t = (Wl/\pi r^2)\{6.78/\sigma + [46/\sigma^2 + 6.4l/(r\sigma E \tan\alpha)]^{1/2}\} \quad (8)$$

The pressure required in the brace is described by

$$p = \sigma t/r \quad (9)$$

Table 2 presents assumed design parameters for X-brace parachutes for Arcas and Dart payload delivery systems. Figure 8 shows corresponding curves for parachute projected area A and mass m_p and for brace tube radius r vs ϵ.

The minimum parachute masses m_p occur at low solidities, between $\epsilon = 0.2$ and $\epsilon = 0.3$. Table 3 presents corresponding system sizes and masses for $\epsilon = 0.2$.

Figure 1 also illustrates a toroid parachute as an alternative to the X-brace design. The toroid is a Mylar tube. The canopy has circular symmetry, and its meridional shape has the form of a modified catenary. The apex is pulled in by a suspension line. The payload is suspended from a number of lines equally spaced on the toroidal brace tube, which is designed to carry a continuous and constant distribution of in-plane compressive forces. If the canopy rise angle at the toroid is greater than zero, and if the number of the suspension lines along the circumference is finite, then the cross sections of the toroid also experience moments in bending and in torsion. Weight minimization procedures for the toroid parachute lead to weights and tube sizes of the brace similar to, but slightly heavier than the X-brace design.

Packaging the Stokes-Flow Parachute

Packaging problems of the large canopy characteristic of the Stokes-flow design were investigated with several series of experimental model parachutes of typical Dart size. Figures 9 and 10 show examples of an X-brace and a toroid parachute, each having a projected canopy area of 9.7 m². The meshes are made of ¼-mil Mylar and they have a solidity of $\epsilon = 0.2$. The X-brace canopy is fabricated in four separate sails having a canopy rise angle of 25°. The toroidal canopy consists of eight identical flat gores. Its central suspension line carries one-half of the total system weight W as selected from tradeoff studies[4] in an effort to minimize parachute mass.

Table 3 Sizes and masses for Stokes-flow decelerators using design parameters of Table 2 and Fig. 8; solidity $\epsilon = 0.2$; $C_D = 0.7$

Parameter	Arcas	Dart
Projected area of canopy A, m²	49	9.7
Surface area of canopy A', m²	56	11.5
Brace tube radius r, cm	5.3	1.9
Internal pressure p, torr	32	58
Parachute mass m_c, kg	0.5	0.06
Payload mass m_p, kg	2.0	0.43
System mass m, kg	2.5	0.49

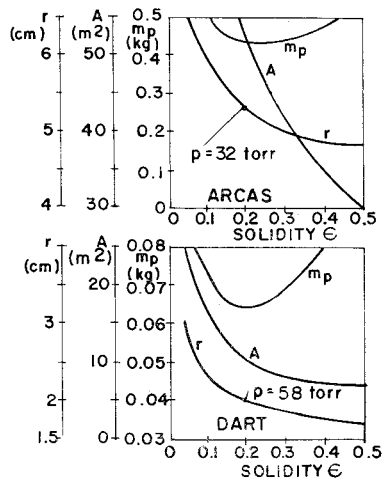

Fig. 8 Canopy sizes and masses, and radii of brace tubes for X-brace parachutes.

Several packaging schemes were investigated, and some guidelines for packaging were established:

1) In order to prevent tearing of the canopy by suspension lines during deployment, no suspension lines should be packaged within the canopy. This requirement places major portions of the brace material at the bottom of the package.

2) A constant density throughout the packaged parachute is desirable, with the brace material distributed evenly.

3) Deployment action should spread from the outer portions of the canopy toward the center, implying that the pressurizing medium is supplied from the brace ends. This procedure also favors evacuation of air from the braces during the packaging process.

4) The braces should be packaged with the fewest possible creases to minimize the occurrence of pin holes at intersections of creases.

Strict adherence to all of these guidelines in one packaging scheme is not possible; therefore some compromise has been involved in each of the methods considered. One successful sequence, known as the "composite" packaging scheme, is shown in Fig. 11.

All the experimental parachute models have been successfully packaged, using the composite or alternative methods,

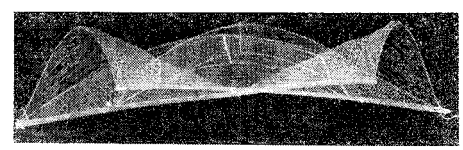

Fig. 9 X-brace parachute for Dart (A = 9.7 m²).

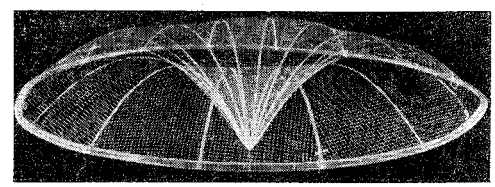

Fig. 10 Toroid parachute for Dart (A = 9.7 m²).

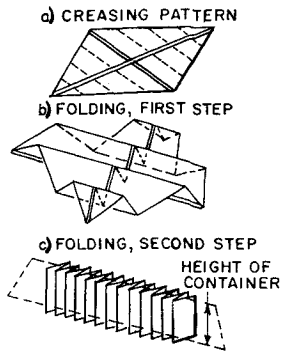

Fig. 11 Folding pattern of X-brace parachute.

within a diameter of 25 mm and a length of 320 mm between the staves of the Dart container. The average packaging density was approximately 0.3 g/cm³ (or 19 lb/ft³).

Experimental Tests

Experimental testing of the Stokes-flow concept has so far been limited to drop tests with subscale models, to verify aerodynamic performance, and to deployment tests with Dart-size experimental parachute models shown in Figs. 9 and 10. These tests were conducted in the 60-ft vacuum facilities at the NASA Langley Research Center.‡

The drop-test models had a side length of 1 m. The canopies consisted of $\frac{1}{4}$-mil aluminized Mylar tapes, 2.5 mm wide, with three different solidities, $\epsilon = 0.5$, 0.1, and 0.2. The same Mylar material was used for the braces, which have a diameter of 9.5 mm. The braces were inflated with residual air. The models were released from the top of the chamber, and their falls were photographically recorded over a distance of approximately 6 m. The canopies were dropped as "wind-drifters" without carrying a payload.

The drop tests were performed at three different pressure altitudes, thereby including a variation in Reynolds number. The results (Fig. 12) follow the trends predicted by theory, but the measured drag coefficients at low Reynolds numbers are slightly better than the theoretical predictions. These drop tests indicated excellent aerodynamic stability of the canopies with no visible tendency to drift.

Deployment tests of Dart-size parachutes confirmed that the packaging schemes developed are workable. Starting with packaging densities of about 0.3 g/cm³, the parachutes were deployed from Dart compartments. The internal pressure in the braces was provided by vaporization of a liquid (Freon 11, methanol). The parachutes generally started to deploy immediately upon release and without major damage to the canopy meshes. The major problem was an excessive

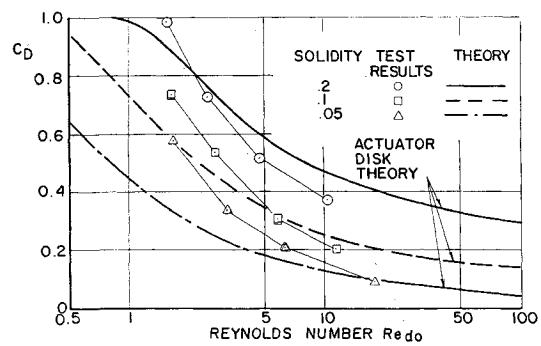

Fig. 12 Experimental drag coefficients for subscale X-brace parachute models.

‡ These experiments were performed at the Langley Research Center under the direction of H. B. Tolefson. The author wishes to express appreciation for permission to refer herein to the test results.

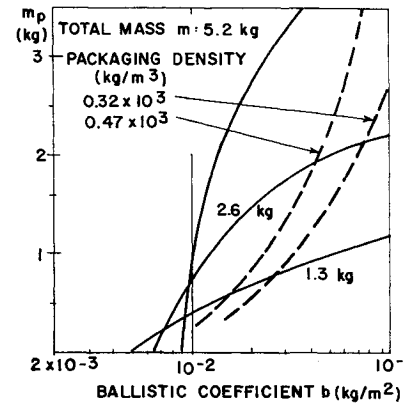

Fig. 13 Payload limits for X-brace parachute.

occurrence of pin holes in the braces; consequently, they did not fully erect because of excessive losses of pressure through the pin holes.

Performance Limits

A principal aim in the development of the Stokes-flow decelerator is the achievement of a minimum ballistic coefficient b for a payload delivery system to perform a specified mission. For an Arcas payload delivery system using an X-brace parachute designed according to current practices, Fig. 13 shows estimated payload masses m_p vs b for total system masses m of 1.3, 2.6, and 5.2 kg. For a given m_p, b is decreased by increasing the size of the parachute, which also increases its mass. The minimum b is reached as the packaging density of the parachute is maximum for a given packaging technique. A parachute can be hand-packaged up to a density of approximately 0.32 g/cm³ (20 lb/ft³). Higher densities, e.g., 0.47 g/cm³ (30 lb/ft³) are possible if pressure packaging techniques are applied. As the size of the parachute increases further, the parasitic weight of the braces increases faster than the drag-producing area. Eventually the parachute becomes too heavy for its size. This limit occurs when the parachute is approximately five times heavier than the payload. This limit is, however, difficult to reach because a packaging density as high as the material itself would be required.

The design data in Tables 2 and 3 represent the current status in the development of the Stokes-flow decelerator.

References

[1] Whitlock, C. H. and Murrow, H. N., "Performance Characteristics of a Preformed Elliptical Parachute at Altitudes between 200 000 and 100 000 Feet Obtained by In-flight Photography," TN D-2183, 1964, NASA.

[2] Eckstrom, C. V., "Development and Testing of the Disk-Gap-Band Parachute Used for Low Dynamic Pressure Applications at Ejection Altitudes at or above 200 000 Feet," CR-502, 1966, NASA.

[3] Graham, J. J., "Ballute Development for Loki-Dart and Arcas Rocket Sondes," Rept. AFCRL-68-0622, 1968, Air Force Cambridge Research Labs., Bedford, Mass.

[4] Niederer, P. G., "Development of a High-Altitude Decelerator," CR-66755, 1969, NASA.

[5] U.S. Patent 3 386 692, June 4, 1968.

[6] Rauscher, M., *Introduction to Aeronautical Dynamics*, Wiley, New York, 1953, pp. 170–174.

[7] Lamb, H., *Hydrodynamics*, 6th ed., Dover, New York, 1932, pp. 614–617.

[8] Hoerner, S. F., *Fluid Dynamic Drag*, published by the author, 1965, p. 3–15.

[9] Schaaf, S. A. and Chambré, P. L., *Flow of Rarefied Gases*, Princeton University Press, Princeton, N.J., 1961, pp. 19–21.

[10] Tsien, H.-S., "Superaerodynamics, Mechanics of Rarefied Gases," *Journal of the Aeronautical Sciences*, Vol. 13, No. 12, Dec. 1946, pp. 653–664.